Table 1
In vitro neurotropism of rHEP and rHEP$^{333}$R

| Strain | Titer (ffu/ml[a]) | | In vitro neurotropism index[b] |
|---|---|---|---|
| | NA | BHK | |
| rHEP | $1.0 \times 10^8$ | $1.0 \times 10^8$ | 0.0 |
| rHEP$^{333}$R | $3.5 \times 10^8$ | $1.1 \times 10^7$ | 1.5 |
| LEP-Flury | $1.0 \times 10^7$ | $2.0 \times 10^5$ | 1.7 |
| CVS | $1.5 \times 10^8$ | $4.5 \times 10^6$ | 1.5 |

[a] Each virus was titrated in NA or BHK-21 cells.
[b] The in vitro neurotropism index is expressed with the logarithm of the titer in NA cells minus the logarithm of the titer in BHK-21 cells.

strains. In addition, the pH threshold for low pH-dependent fusion activity, which was responsible for the entry of virus from endosome to cytoplasm of cell, was not affected by the single amino acid change. These two viruses induced the fusion in BHK-21 cells when the cells were exposed below pH 5.8 (data not shown). Table 1 shows the in vitro neurotropism index of rabies strains, which is indicated as infectivity ratio of the virus in NA cells versus in BHK-21 cells (Morimoto et al., 1998). The value of ratio 1.0 indicates that the virus has 10 times stronger infectivity to neuronal cells than that to non-neuronal cells. Pathogenic rabies strains commonly exhibited higher in vitro neurotropism than attenuated strains did. The index of the pathogenic strain was generally over 1.0, whereas the index of the attenuated strain decreased to be around 0 (Morimoto et al., 1998, 2000; Ito et al., 2001). The indices of rHEP and rHEP$^{333}$R showed 0 and 1.5, respectively. The index of rHEP$^{333}$R increased similar to those of pathogenic LEP-Flury and CVS strains.

### 3.2. Pathogenicity of rHEP$^{333}$R to adult mice

In order to determine the pathogenicity of rHEP and rHEP$^{333}$R in adult mice, $10^5$ ffu of each virus were inoculated intracerebrally. The rHEP-infected mice showed mild symptoms with slight reduction of body weight (Fig. 2A). On the other hand, the mice inoculated with rHEP$^{333}$R showed clinical symptoms indicative of the CNS disease, such as paralysis and hyperactivity. All of the mice inoculated with rHEP$^{333}$R died within 11 days post-infection (dpi). This result clearly shows that the rHEP$^{333}$R increased its pathogenicity in adult mice by a single amino acid change. The $LD_{50}$ of rHEP$^{333}$R was determined, and it was calculated that 154 ffu of rHEP$^{333}$R was required for one $LD_{50}$. The rHEP did not cause death even when $10^6$ ffu of the virus were inoculated. Thus, the ffu required for one $LD_{50}$ was calculated as more than $10^6$ ffu. Highly pathogenic CVS strain required 1.5 ffu for one $LD_{50}$ (data not shown), indicating that rHEP$^{333}$R was 100-times less virulent than the CVS strain. Peripheral pathogenicity was assessed with intramuscular inoculation of mice with rHEP, rHEP$^{333}$R, or CVS strain. None of the mice inoculated intramuscularly with either rHEP or rHEP$^{333}$R died, although one of the six mice inoculated with rHEP$^{333}$R exhibited hind leg paralysis (Fig. 2B). The CVS strain exhibited high in vivo neuroinvasiveness. The in vivo neuroinvasiveness was not increased by the shift to arginine at position 333 in the G protein of HEP-Flury strain.

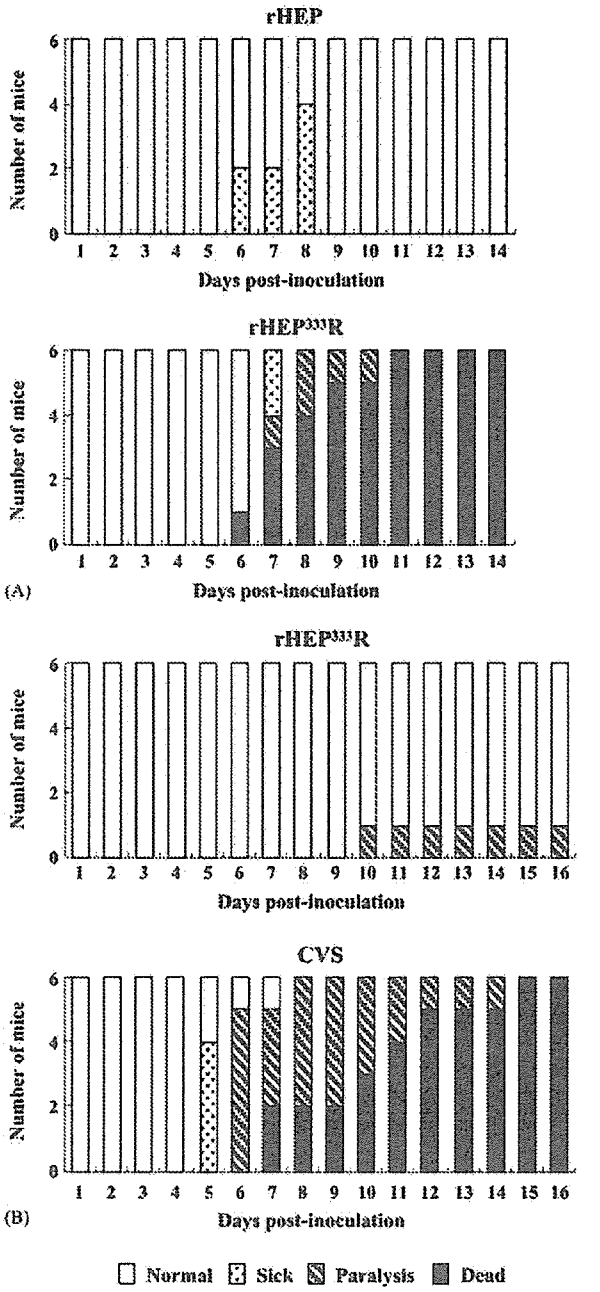


Fig. 2. Mortality and morbidity of mice infected with rabies virus. Six ICR mice were inoculated intracerebrally with $10^5$ ffu of rHEP or rHEP$^{333}$R (A) and were inoculated intramuscularly with $10^7$ ffu of rHEP$^{333}$R or $10^6$ ffu of CVS (B). The infected mice were observed for clinical signs of rabies for 14 days (A) or 16 days (B).

### 3.3. Virus propagation in mouse brains and VNA in the mouse sera

Next, the in vivo properties of rHEP and rHEP$^{333}$R were compared for virus titer, genome replication, antigen distribution, and VNA titer (Fig. 3). Virus titer of the rHEP was not detected during the observation period, whereas virus titer of the rHEP$^{333}$R was $10^{4.65}$ ffu per brain at 4 dpi and increased to a

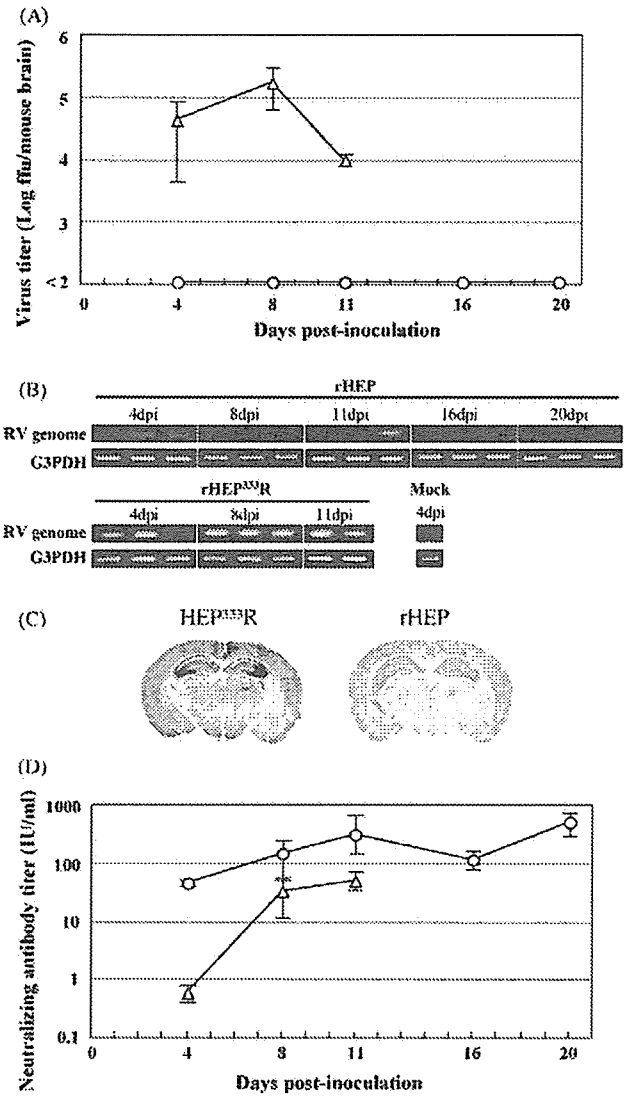


Fig. 3. Virus propagation of rHEP and rHEP$^{333}$R in infected mouse brains: (A) virus titer of rHEP and rHEP$^{333}$R in the infected mouse brains. (B) RT-PCR analysis of viral genome in the infected mouse brains. (C) Immunohistochemical analysis for rabies virus N protein. (D) Anti-rabies neutralizing antibody titers in sera of the infected mice. C57BL/6 mice were infected intracerebrally with $10^5$ ffu of rHEP (open circle) or rHEP$^{333}$R (open triangle). Brains and sera of the infected mice were collected at 4, 8, 11, 16, and 20 dpi. The virus titers were determined by focus forming assay, and shown as titers in total of brain suspension. The RT-PCR analysis was performed with rabies genomic RNA and G3PDH mRNA in the 10% mouse brain emersions. At 4 days after inoculation, the mice were perfused, and the brains were subjected for immunohistochemistry with anti-rabies N antibody. Left side, rHEP$^{333}$R; right side, rHEP. The titers of VNA were expressed as geometric means ± standard errors ($n = 3$).

peak of $10^{5.25}$ ffu per brain at 8 dpi (Fig. 3A). All mice inoculated with rHEP$^{333}$R were dead within 11 dpi.

The viral genomic RNA in the mouse brains was examined by an RT-PCR analysis (Fig. 3B). The band specific for rabies N gene amplified from the genomic sense RNA was detected in the brains inoculated with rHEP$^{333}$R at 4, 8, and 11 dpi. In contrast, weak signal of N gene in the brains inoculated with rHEP was detected at 4 dpi, and disappeared at 8 dpi, while weak signal remained in one of the three brains at 11 dpi. The infectious rHEP viruses were not detected in the brains during the observation period through 20 dpi (Fig. 3A).

The propagation of virus in the brain was also investigated by immunohistochemical analysis for rabies virus N protein. The brain inoculated intracerebrally with either rHEP or rHEP$^{333}$R was removed at 4 dpi and stained with anti-rabies N antibody. As shown in Fig. 3C, antigen-positive cells were presented mainly in the CA3 region of hippocampus of the rHEP$^{333}$R-infected mouse brain, whereas no apparent antigen-positive cells were detected in the rHEP-infected mouse brain.

VNAs play an important role in protection of rabies infection. Titers of the VNA in sera of the mice inoculated with either rHEP$^{333}$R or rHEP were compared (Fig. 3D). Rapid induction of the antibody response was detected in sera of the rHEP-infected mice. The titers were 45 IU/ml at 4 dpi, and increased to 500 IU/ml at 11 dpi. The titers remained high level during the observation period though 20 dpi. On the other hand, titers of the VNA in sera of the mice inoculated with rHEP$^{333}$R were low (0.6 IU/ml) at 4 dpi. Although the titers increased to 34 IU/ml at 8 dpi, all of the mice infected with rHEP$^{333}$R died at 11 dpi. The VNA could not overcome propagation of the rHEP$^{333}$R at the late stage of infection.

### 3.4. Neuronal transport of virus in rat brain

A standard intracerebral inoculation with large inoculum of virus breaks blood–brain barrier and stimulates immune responses in the host. To exclude a possibility that the rapid induction of VNA might prohibit spread of the rHEP strain, stereotaxic inoculation of the viruses into hippocampus dentate gyrus region of the rat brain was performed, which induced much less immune responses (Yang and Jackson, 1992). The spread of the virus was examined at the early stage of infection (36 hpi), and differences of axonal transport in the CNS were assessed (Fig. 4). In inoculation with the rHEP$^{333}$R, spread of antigen-positive cells was observed in the hippocampus CA1 and CA3 regions (Fig. 4D), and lateral entorhinal cortex (LEA) and medial entorhinal cortex (MEA) regions (Fig. 4E, F, respectively). Neurons in LEA and MEA are known to project into hippocampus. In contrast, no antigen-positive cells were detected around the injected site and in LEA and MEA regions of the rHEP-inoculated rat brain. These observations supported that rHEP$^{333}$R gained an ability of axonal transport in the CNS as shown in Kelly and Strick (2000).

## 4. Discussion

The G protein of rabies virus is related to cell attachment (Lentz et al., 1982; Thoulouze et al., 1998; Tuffereau et al., 1998; Yan et al., 2002), induction of apoptosis (Jackson and Rossiter, 1997; Morimoto et al., 1999; Prehaud et al., 2003), and immune responses (Wiktor et al., 1973; Cox et al., 1977; Perrin et al., 1985). Therefore, the G protein plays the most important role in its pathogenicity. An amino acid at position 333 in the G protein has been shown to be critical to the pathogenicity in adult mice (Dietzschold et al., 1983; Seif et al., 1985; Tuffereau et al.,

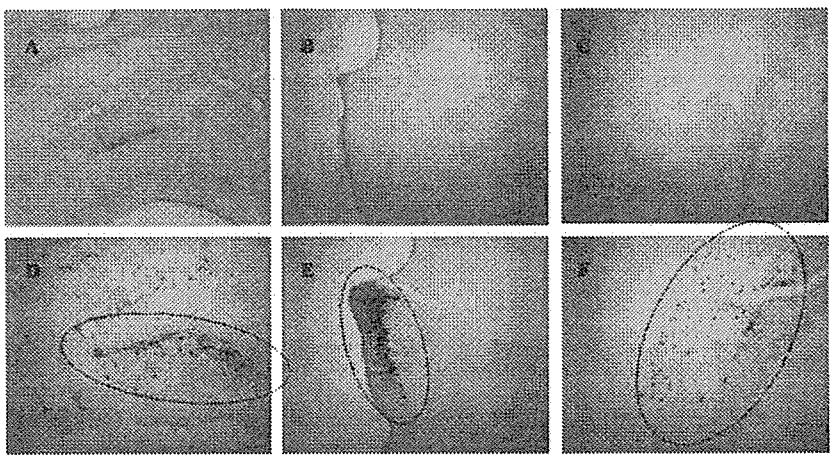

Fig. 4. Retrograde axonal transport of rHEP$^{333}$R in virus-infected rat brains. Wistar rats were infected with $10^4$ ffu of rHEP (A–C) or rHEP$^{333}$R (D–F). The viruses were infected with the stereotaxic inoculation at hippocampus dentate gyrus region. At 36 h after inoculation, the rats were sacrificed for immunohistochemistry with anti-rabies N antibody. Brown signals indicated the rabies virus-antigen positive cells. Pontamine sky blue diffused around the injection site. (A, D) hippocampus region around the injection site. (B, E) lateral entorhinal cortex (LEA), (C, F) medial entorhinal cortex (MEA) projects to the injection site.

1989). However, it has been reported that the other positions were also responsible for the pathogenic shift (Takayama-Ito et al., 2004). This study revealed that an arginine at position 333 increased pathogenicity of a highly attenuated HEP-Flury strain. The rHEP$^{333}$R spread through retrograde axonal transport and propagated efficiently in the CNS, while the parental rHEP did not.

As cellular receptors of rabies virus, a nicotinic acetylcholine receptor (Lentz et al., 1982), a neural cell adhesion molecule (NCAM) (Thoulouze et al., 1998), and a low-affinity neurotrophin receptor p75NTR (Tuffereau et al., 1998) have been reported. An ability of the G protein to bind p75NTR was dependent on the presence of lysine or arginine at positions 330 or 333 (Tuffereau et al., 1998). Thus, this molecule might be responsible for an ability of rHEP$^{333}$R to spread and propagate in the CNS. As shown in Table 1, a significant difference of in vitro neurotropism was found between rHEP and rHEP$^{333}$R, suggesting that the arginine at position 333 altered binding property of the virus into cell species. Pathogenic viruses commonly exhibited higher in vitro neurotropism (Morimoto et al., 1998, 2000; Ito et al., 2001). It might indicate that the receptor usage of rabies virus was shifted to more neurotropic state. CVS strain are able to invade the CNS from a peripheral site and killed mice, whereas other less pathogenic strains such as PV, ERA or rHEP$^{333}$R do not kill mice and rarely induce flaccid hind leg paralysis by a peripheral route of inoculation (Smith, 1981; Galelli et al., 2000). In this regard, it was shown that the arginine at position 333 is not responsible for in vivo neuroinvasiveness of HEP-Flury strain.

The single amino acid substitution at position 333 dramatically altered the ability of the rHEP strain to spread in the CNS through retrograde axonal transport (Fig. 4). Yan et al. (2002) have reported that mutants with glutamine at position 333 in CVS and its derivative strains (CVS-N2c, CVS-B2c) did not change the distribution pattern of the virus spread in the CNS, however, that the same mutant of SN-10 strain lost an ability of the virus to spread in the CNS. It is, therefore, likely that involvement of the amino acid at position 333 for viral spread in the CNS was dependent on the strains. The attenuation of HEP-Flury strain was similar to the attenuation by replacement of the arginine in SN-10 strain.

Intracerebral injection of virus disturbs the immune state of the CNS and stimulates the immune responses. However, stereotaxic inoculation stimulates much less induction of immune responses. Yang and Jackson (1992) have indicated these avirulent mutants of the CVS strain lost virulence after intracerebral inoculation but remained neurovirulent after stereotaxic inoculation. Therefore, they suggested a balance between the spreading efficiency of the virus in the CNS and the level of immune stimulation in the host would determine the pathogenicity (Yang and Jackson, 1992). The avirulent HEP-Flury (rHEP) and the SN-10$^{333}$Gln mutant were incapable to spread in the CNS even after stereotaxic inoculation. In this case, therefore, it was excluded that the rapid induction of VNAs could prevent the rHEP to propagate in the early stage of infection.

There are two proposed models for spread of rabies virus; one is into contiguous cells by neuron-to-neuron transmission, and the other is into noncontiguous cells by free virions (Dietzschold et al., 1985). The neuron-to-neuron transmission through synapse junction would be preferentially utilized in the CNS. In the case of HEP-Flury or SN-10 strain, arginine at position 333 may be critical for the neuron-to-neuron transmission.

VNA is the most important factor in clearance of rabies virus from the CNS (Dietzschold et al., 1992; Hooper et al., 1998). The mice inoculated with rHEP exhibited rapid induction of VNAs without efficient propagation of the virus in the brain. On the other hand, efficient virus propagation was detected in the mouse brains infected with rHEP$^{333}$R, and the induction of VNAs against rHEP$^{333}$R was slower than that of rHEP. The rapid spread of rHEP$^{333}$R in neuron-to-neuron through connecting synapses could retard the immune responses at the early stage of infection. A high level of virus propagation and massive distribution of rHEP$^{333}$R might impair the rapid immune responses

in the CNS. The presence of VNAs at the late stage of infection reduced the infectious rHEP$^{333}$R, but did not clear the virus completely, and the mice did not overcome death from rabies (Fig. 3). Several researchers (Coulon et al., 1982; Marcovistz et al., 1994; Irwin et al., 1999) have observed that the VNA response was faster and higher in avirulent mutant RV194-2 or AvO1 strain infected mice compared to mice infected with CVS strain. These data suggest immune responses of the host against rabies virus were different between pathogenic and avirulent strains.

The G proteins of avirulent viruses induced apoptosis more strongly than those of highly pathogenic viruses in the infected neuron (Morimoto et al., 1999; Prehaud et al., 2003), and the apoptosis consequently evoked higher immune response (Pulmanausahakul et al., 2001; Faber et al., 2002). Resident cells in the CNS might differently induce innate immunity and the following immune responses in an abortive infection or a productive infection. The rHEP having lower in vitro neurotropism might more easily attach to immunocompetent nonneuronal cells than the rHEP$^{333}$R having higher in vitro neurotropism. In addition, it has been reported that suppression of T cell-mediated immune response was caused by infection with pathogenic rabies viruses (Wiktor et al., 1977; Perrin et al., 1996) and might be due to an induction of apoptosis in T cells (Baloul et al., 2004). However, this immune suppression against rabies infection remains to be clarified. Further studies analyzing the differences in immune response induced by rHEP and rHEP$^{333}$R infections are needed to elucidate why rHEP infection induced the VNA so rapidly and efficiently or how rHEP$^{333}$R infection retarded the induction of immune response although the virus had been propagated in the CNS.

In conclusion, we demonstrated here direct evidences that virulence the of the HEP-Flury strain was gained by a single point mutation to arginine at position 333 in the G protein and that the amino acid was responsible for a change of in vitro neurotropism and an ability of the virus to spread by retrograde axonal transport and propagate in the CNS.

## Acknowledgements

This work was supported by grants from the Research on Emerging and Reemerging Infectious Diseases, Ministry of Health, Labor and Welfare, Japan.

## References

Baloul, L., Camelo, S., Lafon, M., 2004. Up-regulation of Fas ligand (FasL) in the central nervous system: a mechanism of immune evasion by rabies virus. J. Neurovirol. 10, 372–382.

Coulon, P., Rollin, P., Blancou, J., Flamand, A., 1982. Avirulent mutants of the CVS strain of rabies virus. Comp. Immunol. Microbiol. Infect. Dis. 5, 117–122.

Coulon, P., Derbin, C., Kucera, P., Lafay, F., Prehaud, C., Flamand, A., 1989. Invasion of the peripheral nervous systems of adult mice by the CVS strain of rabies virus and its avirulent derivative AvO1. J. Virol. 63, 3550–3554.

Cox, J.H., Dietzschold, B., Schneider, L.G., 1977. Rabies virus glycoprotein. II. Biological and serological characterization. Infect. Immun. 16, 754–759.

Dietzschold, B., Wunner, W.H., Wiktor, T.J., Lopes, A.D., Lafon, M., Smith, C.L., Koprowski, H., 1983. Characterization of an antigenic determinant of the glycoprotein that correlates with pathogenicity of rabies virus. Proc. Natl. Acad. Sci. U.S.A. 80, 70–74.

Dietzschold, B., Wiktor, T.J., Trojanowski, J.Q., Macfarlan, R.I., Wunner, W.H., Torres-Anjel, M.J., Koprowski, H., 1985. Differences in cell-to-cell spread of pathogenic and apathogenic rabies virus in vivo and in vitro. J. Virol. 56, 12–18.

Dietzschold, B., Kao, M., Zheng, Y.M., Chen, Z.Y., Maul, G., Fu, Z.F., Rupprecht, C.E., Koprowski, H., 1992. Delineation of putative mechanisms involved in antibody-mediated clearance of rabies virus from the central nervous system. Proc. Natl. Acad. Sci. U.S.A. 89, 7252–7256.

Etessami, R., Conzelmann, K.K., Fadai-Ghotbi, B., Natelson, B., Tsiang, H., Ceccaldi, P.E., 2000. Spread and pathogenic characteristics of a G-deficient rabies virus recombinant: an in vitro and in vivo study. J. Gen. Virol. 81, 2147–2153.

Faber, M., Pulmanausahakul, R., Hodawadekar, S.S., Spitsin, S., McGettigan, J.P., Schnell, M.J., Dietzschold, B., 2002. Overexpression of the rabies virus glycoprotein results in enhancement of apoptosis and antiviral immune response. J. Virol. 76, 3374–3381.

Galelli, A., Baloul, L., Lafon, M., 2000. Abortive rabies virus central nervous infection is controlled by T lymphocyte local recruitment and induction of apoptosis. J. Neurovirol. 6, 359–372.

Gaudin, Y., Ruigrok, R.W., Tuffereau, C., Knossow, M., Flamand, A., 1992. Rabies virus glycoprotein is a trimer. Virology 187, 627–632.

Hooper, D.C., Morimoto, K., Bette, M., Weihe, E., Koprowski, H., Dietzschold, B., 1998. Collaboration of antibody and inflammation in clearance of rabies virus from the central nervous system. J. Virol. 72, 3711–3719.

Inoue, K., Shoji, Y., Kurane, I., Iijima, T., Sakai, T., Morimoto, K., 2003. An improved method for recovering rabies virus from cloned cDNA. J. Virol. Methods 107, 229–236.

Inoue, S., Sato, Y., Hasegawa, H., Noguchi, A., Yamada, A., Kurata, T., Iwasaki, T., 2003. Cross-reactive antigenicity of nucleoproteins of lyssaviruses recognized by a monospecific antirabies virus nucleoprotein antiserum on paraffin sections of formalin-fixed tissues. Pathol. Int. 53, 525–533.

Irwin, D.J., Wunner, W.H., Ertl, H.C., Jackson, A.C., 1999. Basis of rabies virus neurovirulence in mice: expression of major histocompatibility complex class I and class II mRNAs. J. Neurovirol. 5, 485–494.

Ito, H., Minamoto, N., Watanabe, T., Goto, H., Rong, L.T., Sugiyama, M., Kinjo, T., Mannen, K., Mifiine, K., Konobe, T., Yoshida, I., Takamizawa, A., 1994. Aunique mutation of glycoprotein gene of the attenuated RC-HL strain of rabies virus, a seed virus used for production of animal vaccine in Japan. Microbiol. Immunol. 38, 479–482.

Ito, N., Takayama, M., Yamada, K., Sugiyama, M., Minamoto, N., 2001. Rescue of rabies virus from cloned cDNA and identification of the pathogenicity-related gene: glycoprotein gene is associated with virulence for adult mice. J. Virol. 75, 9121–9128.

Jackson, A.C., Rossiter, J.P., 1997. Apoptosis plays an important role in experimental rabies virus infection. J. Virol. 71, 5603–5607.

Kelly, R.M., Strick, P.L., 2000. Rabies as a transneuronal tracer of circuits in the central nervous system. J. Neurosci. Methods 103, 63–71.

Koprowski, H., Black, J., Nelsen, D.J., 1954. Studies on chick-embryo-adapted-rabies virus. VI. Further changes in pathogenic properties following prolonged cultivation in the developing chick embryo. J. Immunol. 72, 94–106.

Kucera, P., Dolivo, M., Coulon, P., Flamand, A., 1985. Pathways of the early propagation of virulent and avirulent rabies strains from the eye to the brain. J. Virol. 55, 158–162.

Lentz, T.L., Burrage, T.G., Smith, A.L., Crick, J., Tignor, G.H., 1982. Is the acetylcholine receptor a rabies virus receptor? Science 215, 182–184.

Marcovistz, R., Leal, E.C., Matos, D.C., Tsiang, H., 1994. Interferon production and immune response induction in apathogenic rabies virus-infected mice. Acta Virol. 38, 193–197.

Mazarakis, N.D., Azzouz, M., Rohll, J.B., Ellard, F.M., Wilkes, F.J., Olsen, A.L., Carter, E.E., Barber, R.D., Baban, D.F., Kingsman, S.M., Kingsman, A.J., O'Malley, K., Mitrophanous, K.A., 2001. Rabies virus glycoprotein

pseudotyping of lentiviral vectors enables retrograde axonal transport and access to the nervous system after peripheral delivery. Hum. Mol. Genet. 10, 2109–2121.

Morimoto, K., Ohkubo, A., Kawai, A., 1989. Structure and transcription of the glycoprotein gene of attenuated HEP-Flury strain of rabies virus. Virology 173, 465–477.

Morimoto, K., Hooper, D.C., Carbaugh, H., Fu, Z.F., Koprowski, H., Dietzschold, B., 1998. Rabies virus quasispecies: implications for pathogenesis. Proc. Natl. Acad. Sci. U.S.A. 95, 3152–3256.

Morimoto, K., Hooper, D.C., Spitsin, S., Koprowski, H., Dietzschold, B., 1999. Pathogenicity of different rabies virus variants inversely correlates with apoptosis and rabies virus glycoprotein expression in infected primary neuron cultures. J. Virol. 73, 510–518.

Morimoto, K., Foley, H.D., McGettigan, J.P., Schnell, M.J., Dietzschold, B., 2000. Reinvestigation of the role of the rabies virus glycoprotein in viral pathogenesis using a reverse genetics approach. J. Neurovirol. 6, 373–381.

Paxinos, G., Watson, C., 1986. The Rat Brain: In Stereotaxic Coordinates, second ed. Academic Press.

Perrin, P., Thibodeau, L., Sureau, P., 1985. Rabies immunosome (subunit vaccine) structure and immunogenicity pre- and post-exposure protection studies. Vaccine 3, 325–332.

Perrin, P., Tino de Franco, M., Jallet, C., Fouque, F., Morgeaux, S., Tordo, N., Colle, J.H., 1996. The antigen-specific cell-mediated immune response in mice is suppressed by infection with pathogenic lyssaviruses. Res. Virol. 147, 289–299.

Prehaud, C., Lay, S., Dietzschold, B., Lafon, M., 2003. Glycoprotein of nonpathogenie rabies viruses is a key determinant of human cell apoptosis. J. Virol. 77, 10537–10547.

Pulmanausahakul, R., Faber, M., Morimoto, K., Spitsin, S., Weihe, E., Hooper, D.C., Schnell, M.J., Dietzschold, B., 2001. Overexpression of cytochrome c by a recombinant rabies virus attenuates pathogenicity and enhances antiviral immunity. J. Virol. 75, 10800–10807.

Reed, L.J., Muench, H., 1938. A simple method of estimating fifty percent end points. Am. J. Hyg. 27, 493–497.

Seif, I., Coulon, P., Rollin, P.E., Flamand, A., 1985. Rabies virulence: effect on pathogenicity and sequence characterization of rabies virus mutations affecting antigenic site III of the glycoprotein. J. Virol. 53, 926–934.

Smith, J.S., 1981. Mouse model for abortive rabies infection of the central nervous system. Infect. Immun. 31, 297–308.

Takayama-Ito, M., Ito, N., Yamada, K., Minamoto, N., Sugiyama, M., 2004. Region at amino acids 164 to 303 of the rabies virus glycoprotein plays an important role in pathogenicity for adult mice. J. Neurovirol. 10, 131–135.

Thoulouze, M.I., Lafage, M., Schachner, M., Hartmann, U., Cremer, H., Lafon, M., 1998. The neural cell adhesion molecule is a receptor for rabies virus. J. Virol. 72, 7181–7190.

Tordo, N., Poch, O., Ermine, A., Keith, G., Rougeon, F., 1986. Walking along the rabies genome: is the large G-L intergenic region a remnant gene? Proc. Natl. Acad. Sci. U.S.A. 83, 3914–3918.

Tuffereau, C., Leblois, H., Benejean, J., Coulon, P., Lafay, E., Flamand, A., 1989. Arginine or lysine in position 333 of ERA and CVS glycoprotein is necessary for rabies virulence in adult mice. Virology 172, 206–212.

Tuffereau, C., Benejean, J., Blondel, D., Kieffer, B., Flamand, A., 1998. Low-affinity nerve-growth factor receptor (P75NTR) can serve as a receptor for rabies virus. EMBO J. 17, 7250–7259.

Wiktor, T.J., Gyorgy, E., Schlumberger, D., Sokol, E., Koprowski, H., 1973. Antigenic properties of rabies virus components. J. Immunol. 110, 269–276.

Wiktor, T.J., Doherty, P.C., Koprowski, H., 1977. Suppression of cell-mediated immunity by street rabies virus. J. Exp. Med. 145, 1617–1622.

Wiktor, T.J., Macfarlan, R.I., Foggin, C.M., Koprowski, H., 1984. Antigenic analysis of rabies and Mokola virus from Zimbabwe using monoclonal antibodies. Dev. Biol. Stand. 57, 199–211.

Yan, X., Mohankumar, P.S., Dietzschold, B., Schnell, M.J., Fu, Z.F., 2002. The rabies virus glycoprotein determines the distribution of different rabies virus strains in the brain. J. Neurovirol. 8, 345–352.

Yang, C., Jackson, A.C., 1992. Basis of neurovirulence of avirulent rabies virus variant Av01 with stereotaxic brain inoculation in mice. J. Gen. Virol. 73, 895–900.

FULL PAPER *Pathology*

# The Histopathogenesis of Paralytic Rabies in Six-Week-Old C57BL/6J Mice Following Inoculation of the CVS-11 Strain into the Right Triceps Surae Muscle

Chun-Ho PARK[1)], Mariko KONDO[1)], Satoshi INOUE[2)], Akira NOGUCHI[2)], Toshifumi OYAMADA[1)], Hiroyasu YOSHIKAWA[1)] and Akio YAMADA[2)]

[1)]*Department of Veterinary Pathology, School of Veterinary Medicine and Animal Sciences, Kitasato University, Towada 034-8628 and* [2)]*Department of Veterinary Science, National Institute of Infectious Diseases, Tokyo 162-8640, Japan*

(Received 8 December 2005/Accepted 21 February 2006)

ABSTRACT. A fatal encephalomyelitis was developed after intracerebral and hind limb inoculation of in 6-week-old C57BL/6J mice by the inoculation of fixed rabies virus (CVS-11 strain), intracerebrally and into hind. After the intracerebral inoculation, virus antigens were detected in the cerebral cortex and hippocampus at 2 days postinoculation (PI), and later spread centrifugally to thalamus, brain stem, cerebellum, spinal cord and spinal ganglia. At 4 days PI, severe apoptosis and DNA fragmentation were observed in the hippocampus and cerebral cortex. All mice infected intracerebrally were dead without limb paralysis at from 10 to 11 days PI. In contrast, mice infected with virus intramuscularly were persistently observed virus antigens in the myocytes at the site of inoculation from 2 days PI. At 4 days PI, the antigens were demonstrated in the spinal dorsal root ganglia, spinal cord and muscle spindles without their detection in the cerebrum and hippocampus. There were no apoptosis in the spinal cord and dorsal root ganglia, however hind limb paralysis was found in all infected mice. Hind limb paralysis was progressed to quadriparalysis, and mice were dead from 11 to 13 days PI. From 4 days PI, necrosis of neuron was observed in the the spinal and dorsal ganglia with infiltration of lymphocyte. This study suggested that the necrosis of spinal neurons was more important to cause the paralysis of hind limb rather than the severe cerebral infection and apoptosis in C57BL/6J mice infected with CVS-11 strain. The virus primarily replicated in the muscles was ascended the spinal cord via afferent fibers and retrogradely invaded the cerebrum, and with subsequent spread to muscle spindles.

KEY WORDS: C57BL/6J mouse, encephalomyelitis, pathogenesis, rabies (CVS-11).

*J. Vet. Med. Sci.* 68(6): 589–595, 2006

Rabies is an ancient disease that is still endemic in many parts of the world. Rabies virus is a neurotropic virus that causes fatal encephalomyelitis in humans and animals [23]; however, the precise invasion routes from the periphery to the central nervous system (CNS) are unknown. It was hypothesized that replication of virus in skeletal muscle might be necessary to generate sufficient virus for entry into the peripheral nervous system [4, 5]. Other studies indicate that the virus can enter nerve terminals directly without replication in muscle [3, 9, 15, 18, 20, 30]. Anatomical analyses of neuronal nuclei infected by rabies virus following peripheral inoculation have demonstrated that the virus propagates in the CNS across chains of synaptically connected neurons [1, 19, 27, 29].

The Challenge Virus Standard (CVS) strain of fixed virus is a pathogenic virus that causes fetal acute myeloencephalitis. In several studies, it was reported that apoptosis plays an important role in pathogenesis of CVS virus infected animals [23]. Apoptosis is considered individual cell death, as it does not induce damage to neighboring cells. In contrast, necrotic cell death, which occurs in response to acute cellular damage, is characterized by cellular alterations that differ from those characteristic of apoptosis, including cell swelling, random degradation of chromatin, and eventually cell lysis [7, 21]. Intracerebrally inoculated rabies virus (CVS strain) caused strong apoptosis in the cerebral cortex and hippocampus in suckling and adult ICR mice [16, 22], while the Purkinje cells of the mouse and rat embryonic spinal motor neurons were more resistant to apoptotic cell death [10, 16]. These reports suggest that various neuronal cell types have susceptibility to rabies virus but that the mechanism of induction of cell death differs among neurons after infection.

In this study, fixed CVS-11 strain was inoculated into the cerebrum and peripheral muscles of adult C57BL/6J mice, and the primary target cells and the sequential involvement of major regions during infection in the peripheral tissues and CNS were investigated. In addition, the patterns of neuronal cell death with time courses in the brain and spinal cord of infected mice were compared.

## MATERIAL AND METHODS

*Virus, animals, and inoculations*: The CVS-11 strain of fixed rabies virus, which was obtained from Dr. C. E. Rupprecht (Rabies Section, Viral and Rickettsia Zoonoses Branch, Center for Disease Control and Prevention, Atlanta, GA, U.S.A.), was replicatedgrown in mouse A/J (H-2a) neuroblastoma cells as previously described [27]. Thirty nine 6-week-old C57BL/6J mice were purchased from Japan SLC, Inc. (Shizuoka, Japan). Intracerebrally (right forebrain), 18 mice were inoculated with viral doses of $10^5$ plaque-forming units of the CVS-11 strain suspended in phosphate-buffered saline (PBS). Whereas, intramuscularly (right triceps surae muscle), 21 mice were inoculated viral doses of $10^5$ and $10^7$ plaque-forming units of the CVS-11 strain suspended in phosphate-buffered saline (PBS). Two groups of 2 uninfected control mice were respectively inoc-

ulated with PBS, intracerebrally and intramuscularly. The inoculated mice were observed daily for neurological conditions and were killed at 2, 3, 4, 5, 7 and 9 days postinoculation (PI)—three to 6 mice per day. All experiments were performed in level-2 biosafety laboratories according to Committees on Biosafety and Animal Handling and Ethical Regulation of the National Institute of Infectious Diseases, Japan. Animal care, breeding, virus inoculation and observation were performed in accordance with the guidelines of Committees.

*Necropsy and preparation of tissue sections*: Each mouse was perfused transcardially with 10–15 m*l* of PBS followed by freshly prepared 4% paraformaldehyde in 0.1 M PBS, pH 7.4. Brains and muscles were removed and postfixed in 4% paraformaldehyde at room temperature for less than 24 hr. The spinal samples were decalcified in K-CX (Fujisawa, Japan) solution after fixation. Coronal sections of the brains at the positions of the olfactory bulb, forebrain, mamillary bodymary and pons and transverse sections of the spinal cords at C2 to C4, T3 to T5, L2 to L4 and S1 to S3 were prepared. Complete series of paraffin sections about 3 $\mu$m thick were cut and mounted on glass slides. Serial sections were used for hematoxylin and eosin (HE) staining, immunohistochemistry and TUNEL assays.

*Immunohistochemistry*: Paraffin sections were mounted on silane-coated slides, deparaffinized in xylene and rehydrated in alcohol, then treated with 0.025% trypsin at 37°C for 30 min. After blocking of endogenous peroxidase activity with 0.3% $H_2O_2$ in methanol for 30 min, sections were treated with 5% normal goat serum to block nonspecific reactions. For detection of rabies virus antigens in the tissues, all sections were stained using the streptavidin-biotin-peroxidase complex (LSAB) method using rabbit anti-CVS-11 strain nucleoprotein at a 1:2,000 dilution as previously described [13]. Tissues from uninfected mice and substitution of normal rabbit serum for the primary antibody were used as controls.

*TUNEL assay*: In order to compare the DNA strand breaks in tissue sections from infected mice, the terminal deoxynucleotidyl transferase mediated dUTP-biotin nick end labeling (TUNEL) method (R & D Systems, Minneapolis, MN) was used. Paraffin sections from infected mice sacrificed at 3, 5, 7 and 9 days PI were prepared according to the manufacturer's instructions. Selected slides were double labeled with the TUNEL method followed by immunostaining for rabies virus antigen without counterstaining.

## RESULTS

*Clinical signs*: The mice became hunched and hypokinetic 4 to 5 days after intracerebral inoculation and subsequently became moribund at 8 days PI. No mice showed paralysis before their death at 10 to 11 days PI. In intramuscularly inoculated mice, paralysis was found at 4 days PI. Paralysis was initially mild with decreased hind limb movement, but as the disease worsened, the mice became severely paralyzed at 7 days PI and progressed to quadriparalysis at 9 days PI. All infected mice died between 11 to 13 days PI.

*Intracerebral inoculation*

*Histology*: No histological changes were observed in any area, including the hippocampus, up to 3 days PI. At 4 days PI, the nuclear pyknosis and fragmentation, cytoplasmic shrinkage were first seen in the pyramidal neurons (CA3, Fig. 1a) of the hippocampus. These findings became severe and most of the pyramidal neurons were destroyed at 7 days PI (Fig. 1b). Lesser changes were observed in multiple other areas, including the thalamus, brain stem and cerebellum at 5 days PI. Throughout the experiments, no histological changes were observed in the neurons of the dentate gyrus of the hippocampus, spinal neurons, spinal ganglia neurons and muscles.

*Immunohistochemistry*: The localization of viral antigens in the cerebral cortex, hippocampus, thalamus, brain stem, cerebellum, spinal cord and muscles is summarized in Table 1. Immunohistochemical examination revealed viral antigens in the right cerebral cortex and hippocampus (CA3) at 2 days PI. In the thalamus, brain stem, spinal cord (cervical, thoracic, lumbar, sacral), spinal dorsal ganglia, small numbers of virus positive neurons were first detected at 4 days PI. Viral antigens were not found in the glial cells in the spinal cord and brain. All of the neurons in the pyramidal layer of hippocampus were positive at 4 days PI (Fig. 1c) and more significant at 7 days PI (Fig. 1d), but neurons in the dentate gyrus was negative. In the cerebellum, antigen positive reactions were found in the Purkinje cells and neurons in the cerebellar nuclei at 5 days PI. At 5 days PI, a small number of positive cells were observed in the muscle spindles around the thoracic vertebrae.

*TUNEL assays*: TUNEL staining of the brain and spinal cord sections showed prominent staining in topographic regions with apoptotic morphologic changes and viral antigen positive cells. TUNEL staining of neurons in the pyramidal layer of the hippocampus was found from 4 days PI (Fig. 1e) and gradually increased as disease progressed. Staining was most prominent in the pyramidal neurons (CA3) at 7 days PI (Fig. 1f). Despite strong immunostaining for the viral antigen in cerebellar Purkinje cells, TUNEL staining was markedly less. No TUNEL staining was found in the dentate gyrus of the hippocampus, spinal cord, spinal ganglia, muscle spindle and muscle fibers.

*Intramuscular inoculation*

*Histology*: In the spinal cord and dorsal root ganglia, chromatolysis, Negri body-like inclusions and necrotic gangliocytes with proliferation of microglial cells, lymphocytes and macrophages were found from 4 days PI, and the numbers of necrotic neurons increased as the paralysis progressed at 7 days PI (Figs. 2a and 2b). In the cerebral cortex, thalamus, brain stem and cerebellum (Fig. 2c), similar histological changes were observed in infected neurons at the terminal stages. In the muscle fibers, at the site of inoculation, hyaline degeneration was found at 2 days PI and mild inflammatory cell infiltrates composed of neutrophils, lymphocytes and macrophages were observed around the small vessels. At 5 days PI, regeneration figures such as nuclear

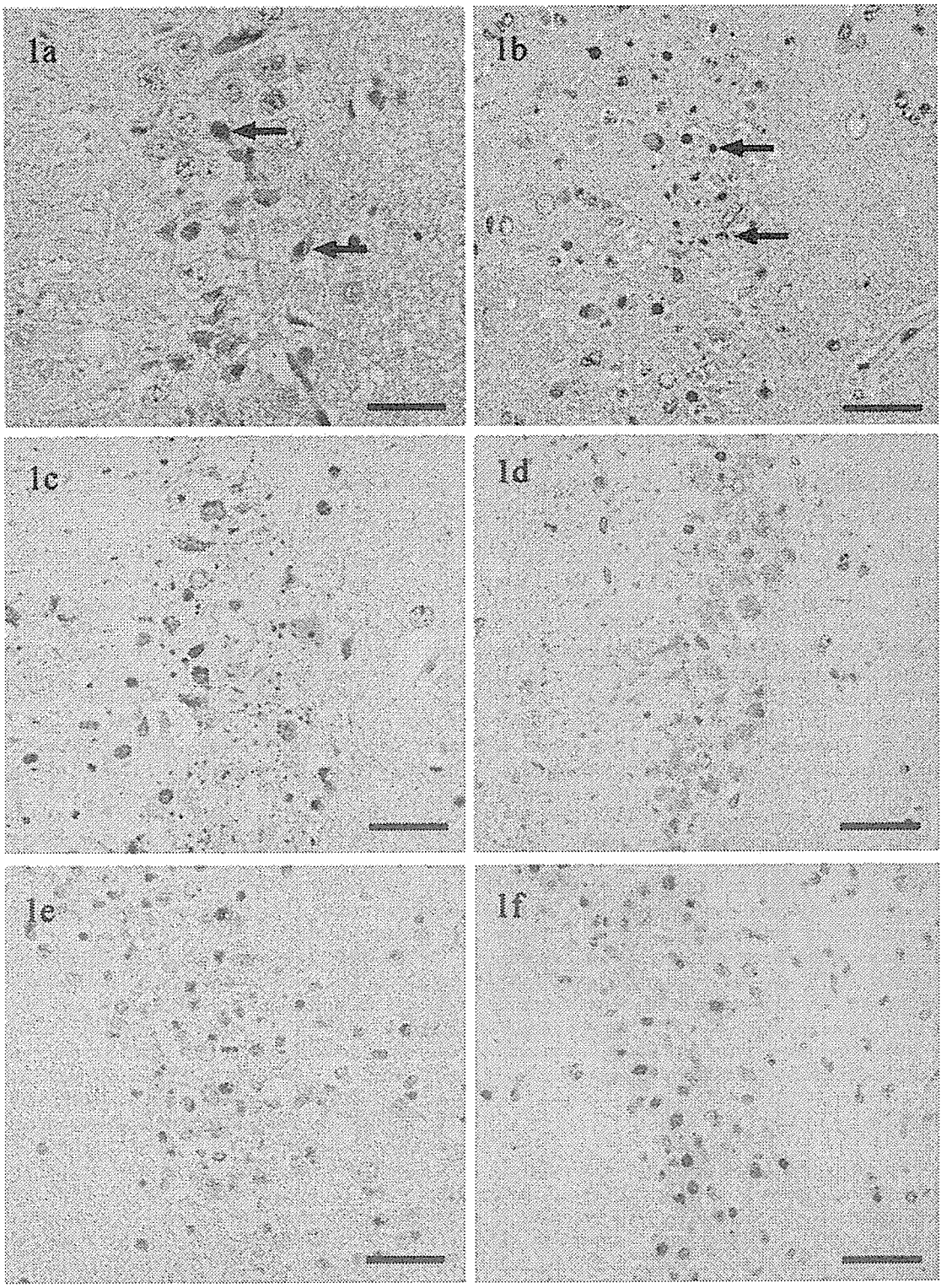


Fig. 1. Hippocampus (CA3). Histology, immunohistochemistry and TUNEL assay of after intracerebral inoculation of CVS-11 at 4 days PI (Figs.1a, c, e) and at 7 days PI (Figs. 1b, d, f). Eosinophilic cytoplasm and nuclear pyknosis (arrows, 1a), viral antigens (1c) and TUNEL positive cells (1e) was observed in pyramidal neurons. Nuclear fragmentation, pyknosis and vacuolation (arrows, 1b) and viral antigens (1d) and TUNEL positive cells (1f) are more significantly observed at 7 days. Bar=30 $\mu$m.

Table 1. Distribution of CVS-11 virus antigens in mice infected intracerebrally

| Days post-inoculation | 2 | 3 | 4 | 5 | 7 | 9 |
|---|---|---|---|---|---|---|
| Organ | | | | | | |
| Brain | | | | | | |
| Cerebral cortex | 1/3* | 3/3 | 3/3 | 3/3 | 3/3 | 3/3 |
| Hippocampus | 1/3 | 2/3 | 3/3 | 3/3 | 3/3 | 3/3 |
| Thalamus | 0/3 | 0/3 | 2/3 | 3/3 | 3/3 | 3/3 |
| Brain stem | 0/3 | 0/3 | 1/3 | 3/3 | 3/3 | 3/3 |
| Purkinje cells | 0/3 | 0/3 | 0/3 | 3/3 | 3/3 | 3/3 |
| Cerebellar nuclei | 0/3 | 0/3 | 0/3 | 3/3 | 3/3 | 3/3 |
| Spinal cord# | | | | | | |
| C | 0/3 | 0/3 | 3/3 | 3/3 | 3/3 | 3/3 |
| T | 0/3 | 0/3 | 3/3 | 3/3 | 3/3 | 3/3 |
| L | 0/3 | 0/3 | 2/3 | 2/3 | 3/3 | 3/3 |
| S | 0/3 | 0/3 | 2/3 | 2/3 | 3/3 | 3/3 |
| Muscle spindles¶ | 0/3 | 0/3 | 0/3 | 1/3 | 2/3 | 3/3 |

*: Number of mice with positive staining for CVS-11 virus antigen/number of total mice used in experiment. #C: cervical, T: thoracic, L: lumbar, S: sacral cord. ¶: Muscle spindles around the infected cervical spinal cord.

chains and proliferating myoblasts were observed (Fig. 3a). No histological changes were found in any area of the hippocampus or muscle spindles throughout the experiments.

*Immunohistochemistry*: The localization of viral antigens in the cerebral cortex, hippocampus, thalamus, brain stem, cerebellum, spinal cord and muscles are summarized in Table 2. Antigen was initially observed in muscles at the site of inoculation in 2 of 3 infected mice at 2 days PI (Fig. 3b). Rarely, antigen positive reactions were also found in the peripheral nerves in the muscles. At 4 days PI, virus positive neurons were observed in the spinal dorsal root ganglia (Fig. 3c), spinal cord (Fig. 3d) and muscle spindles (Fig. 3e) around the sacral spina prior to the cerebrum, thalamus and cerebellum. At 5 days PI, virus positive neurons were detected in the cerebral cortex, thalamus, brain stem and cerebellum. The earliest hippocampal involvement was observed in the CA3 region at 7 days PI.

*TUNEL assay*: TUNEL staining was prominent in the external granular layer and scattered cells in the internal granular cell layer of the cerebellum. However, despite strong immunostaining for rabies virus antigen in cerebellar Purkinje cells, TUNEL staining was markedly less (Fig. 3f). TUNEL staining was not observed in the spinal motor and/or sensory neurons and spinal dorsal root ganglia gangliocytes. Some of the inflammatory cells and glial cells in the spinal cord and brain showed TUNEL staining.

## DISCUSSION

In this study, clinicopathological appearances differed distinctly between intracerebrally and intramuscularly mice infected with the CVS-11 strain. After intracerebral inoculation, hippocampus and cerebral cortex neurons were the initial target, and apoptosis was induced before inflammatory cell infiltration. In addition, a good correlation between the distributions of apoptotic cells and viral antigen positive cells was observed. These findings are supported by the data reported by Jackson *et al.* [16, 17] and Theerasurakarn and Ubol [29].

After hind limb inoculation, a more natural route of viral entry, viral antigen was first detected, and persisted until the terminal stages, in the muscle at the site of inoculation and was then detected in the spinal dorsal root ganglia, spinal cord and muscle spindles. These findings indicate that the virus reached the CNS in a retrograde direction through peripheral sensory nerves following replication in the muscles, and subsequently spread in an anterograde direction to distant muscle spindles. Limb paralysis appeared at the same time as necrotic changes and virus antigens were detected at 4 days PI. However, virus infected spinal motor and/or sensory neurons and spinal ganglion gangliocytes were TUNEL negative despite strong immunostaining. These results are partially in accordance with those of the previous report by Guigoniet *et al.* [10], in which rat embryonic spinal motor neurons and spinal cord of rat neonates were more resistant to cytolysis and apoptosis than hippocampus neurons after CVS strain infection.

In this study, infiltration of inflammatory cells into the muscles at the site of inoculation, the spinal dorsal root ganglia and the spinal cord were observed in early stage of infection. In addition, paralytic signs were distinct in intramuscularly infected mice in spite of less cerebral destruction. Therefore, it was suggested that activation of local immune responses in peripheral muscle and spinal cord, and the dysfunction of infected spinal neurons were precedence of paralytic manifestations. The pathogenesis of rabies includes encephalitis and paralysis [23]. However, little explanation has been provided that would account for these diverse manifestations of infection with a common agent [12]. Immunosuppressed and athymic mice develop encephalitic rabies. This encephalitis occurs concomitantly with increased virus replication and destruction of neurons in the absence of detectable immune mediators [14, 32]. Paralytic rabies is found in immunocompetent mice only.

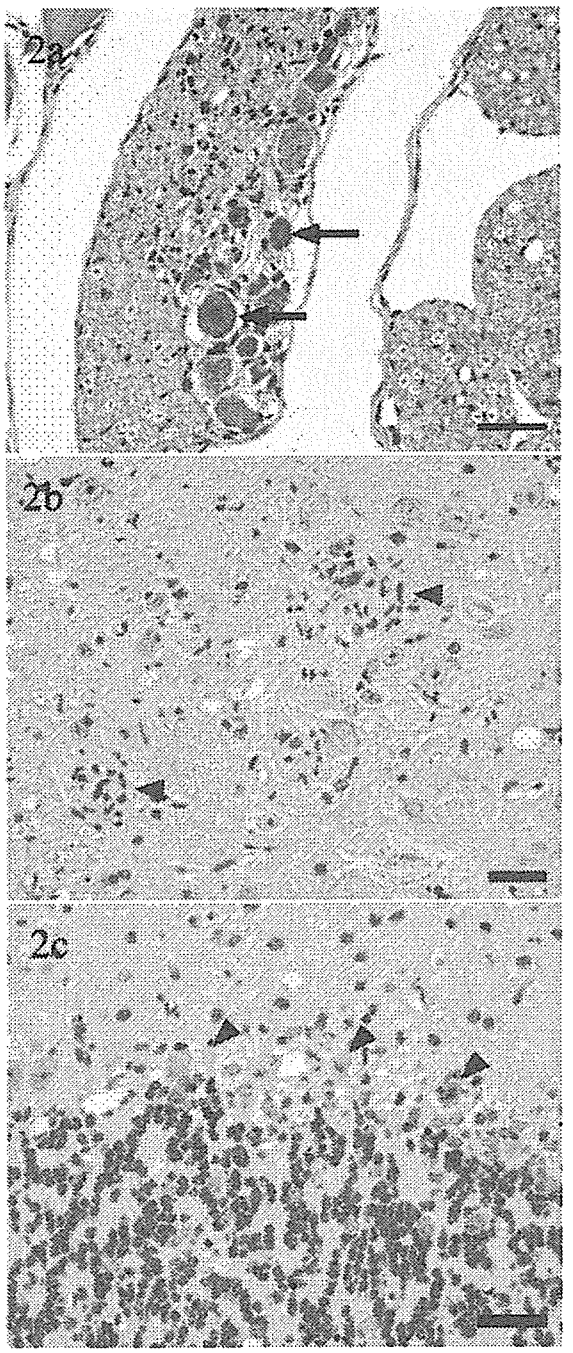


Fig. 2. Intramuscularly infected C57BL/6J mouse. Spinal dorsal ganglions, spinal cord and cerebellum at 7 days PI. Degenerated gangliocytes (arrows, 2a), necrotic spinal neurons with microgliosis (arrowheads, 2b) and necrotic Purkinje cells (arrowheads, 2c) were observed. Bar=30 μm (Figs. 2a and 2c), Bar=50 μm (Fig. 2b).

Passive transfer of immune sera and activated lymphocytes to immunosuppressed mice results in paralysis and early death [14]. In contrast to mice, paralytic rabies in humans has been found with defective immune reactions, while encephalitic rabies cases have an active immune response to rabies. This raises questions as to whether immune responses are significant in rabies pathogenesis and whether the pathogenesis process differs in mice and human.

Table 2. Distribution of CVS-11 virus antigens in mice infected intramuscularly

| Days postinoculation | 2 | 3 | 4 | 5 | 7 | 9 |
|---|---|---|---|---|---|---|
| Organ | | | | | | |
| Brain | | | | | | |
| Cerebral cortex | 0/3* | 0/3 | 0/3 | 1/3 | 6/6 | 3/3 |
| Hippocampus | 0/3 | 0/3 | 0/3 | 0/3 | 3/6 | 2/3 |
| Thalamus | 0/3 | 0/3 | 0/3 | 1/3 | 6/6 | 3/3 |
| Brain stem | 0/3 | 0/3 | 0/3 | 2/3 | 6/6 | 3/3 |
| Purkinje cells | 0/3 | 0/3 | 0/3 | 1/3 | 6/6 | 3/3 |
| Cerebellar nuclei | 0/3 | 0/3 | 0/3 | 1/3 | 6/6 | 3/3 |
| Spinal cord# | | | | | | |
| C | 0/3 | 0/3 | 2/3 | 3/3 | 6/6 | 3/3 |
| T | 0/3 | 0/3 | 2/3 | 3/3 | 6/6 | 3/3 |
| L | 0/3 | 0/3 | 2/3 | 3/3 | 6/6 | 3/3 |
| S | 0/3 | 0/3 | 2/3 | 3/3 | 6/6 | 3/3 |
| Other | | | | | | |
| Muscle spindles¶ | 0/3 | 0/3 | 1/3 | 3/3 | 6/6 | 3/3 |
| Muscle§ | 2/3 | 3/3 | 3/3 | 3/3 | 6/6 | 3/3 |

*: Number of mice with positive staining for CVS-11 virus antigen/ number of total mice used in experiment. #C: cervical, T: thoracic, L: lumbar, S: sacral cord. ¶: Muscle spindles around the infected sacral spinal cord. §: Right triceps surae muscle.

Muscle plays an important role in the pathogenesis of rabies. However, it remains to be determined whether viral replication in muscle is essential for further virus spread. In several experiments, local replication in myocytes after inoculation into muscle seemed to precede the appearance of viral material in the nervous system [4, 5, 11, 24, 25]. In contrast, Coulon *et al.* [8] and Shankar *et al.* [26] did not find any evidence of replication in the muscle, suggesting that the virus could penetrate directly into the nerve endings. The present study supported the former case because viral antigen was initially detected in muscles. Baer *et al.* [2] and Charlton *et al.* [6] reported long incubation periods in muscle of rabid animals. In the present study, viral antigens were persistently detected in muscle at the inoculation site and did not spread directly from one muscle fiber to another.

In this study, viral antigens were detected in spindle muscles at an early stage of infection when infected mice showed paralysis. The virus that initially or subsequently replicated in the spinal cord or spinal ganglia had directly descended to the spindles via sensory or/and motor nerve fibers. Muscle spindles are skeletal muscle mechanoreceptors that mediate the stretch reflex and provide axial and limb position information to the CNS. Spindles consist of encapsulated muscle fibers (intrafusal fibers) that are innervated by specialized sensory and motor neurons. However, we do not know the direct effects of viral infection in spindles on cellular function or paralysis as no evidence that suggested morphological changes was observed until the terminal stage of infection. Therefore, further studies are

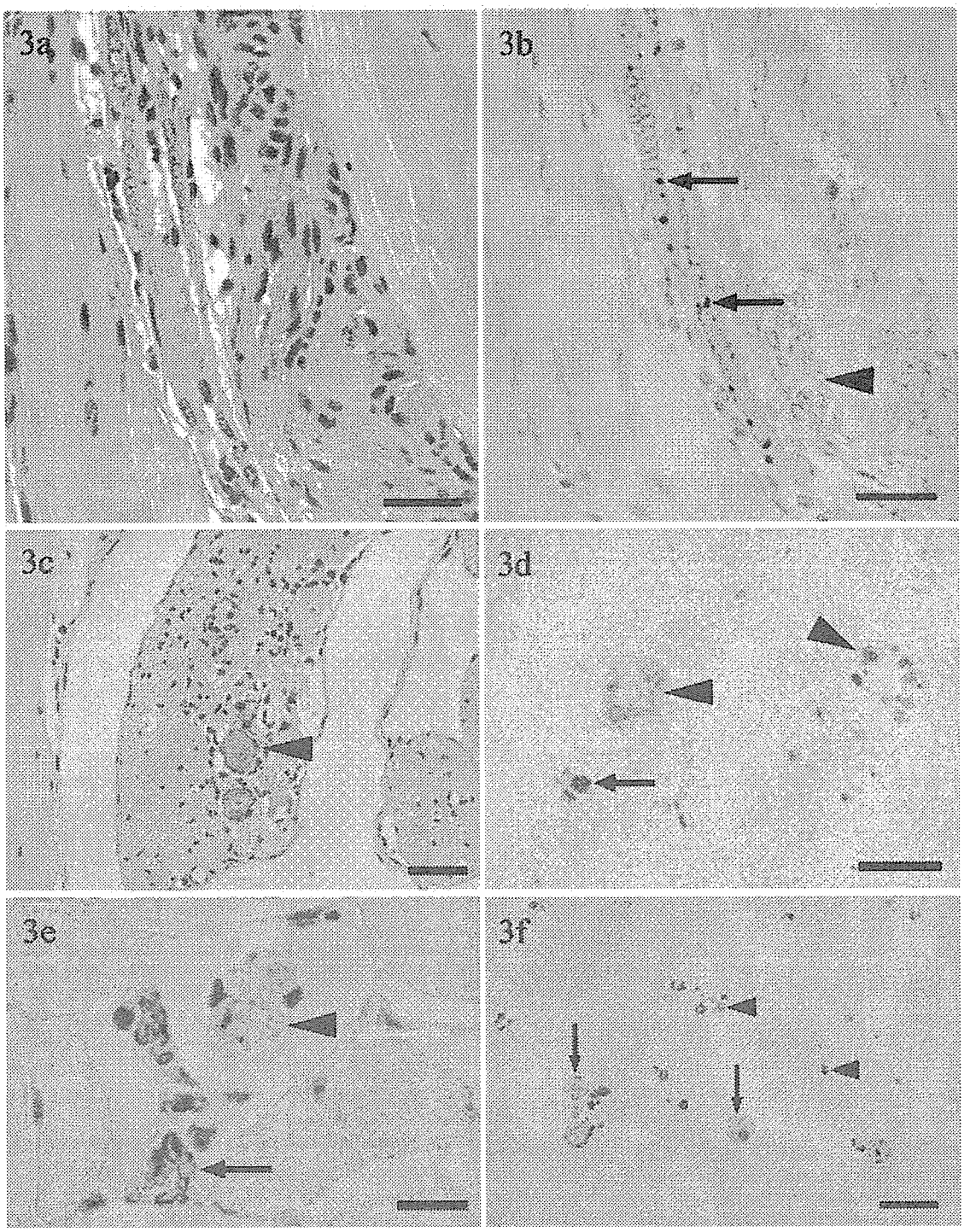


Fig. 3. Intramuscularly infected C57BL/6J mouse. At 5 days PI, hyaline degeneration, nuclear chain indicating muscular regeneration and perivascular infiltration (3a) are observed. Numerous viral antigen spots in the cytoplasm of muscle (arrows, 3b) and weak positive reaction (arrowhead, 3b) are seen in the peripheral nerve system. Viral antigens were observed in the cytoplasm of dorsal root ganglia gangliocytes (arrowhead, 3c). By double staining, viral positive neurons (arrowheads, 3d) and TUNEL positive glial cells (arrow, 3d) are seen. Viral antigens are also seen in the cytoplasm of muscle spindle (arrowhead, 3e) and peripheral nerve system (arrow, 3e). TUNEL staining was observed not only in the external granular cells (arrowheads, 3e) but also Purkinje cells (arrows, 3f). Bar=30 $\mu$m (Figs. 3a, b, c and f), Bar=20 $\mu$m (Figs. 3d and 3e).

required to address the effects of muscle spindle involvement in the clinical magnifications of rabies.

ACKNOWLEDGMENTS. This study was partly supported by a Research on Emerging and Reemerging Infectious Diseases grant from the Ministry of Health, Labor and Welfare of Japan, and a Grant for Scientific Research (Park CH: 2850) from the School of Veterinary Medicine and Animal Sciences of Kitasato University, Japan.

REFERENCES

1. Astic, L., Saucier, D., Coulon, P., Lafay, F. and Flamand, A. 1993. The CVS strain of rabies virus as transneuronal tracer in the olfactory system of mice. *Brain Res.* **619**: 146–156.
2. Baer, G. M. and Cleary, W. F. 1972. A model in mice for the pathogenesis and treatment of rabies. *J. Infect. Dis.* **125**: 520–527.
3. Burrage, T. G., Tignor, G. H. and Smith, A. L. 1985. Rabies virus binding at neuromuscular junctions. *Virus Res.* **2**: 273–289.
4. Charlton, K. M. and Casey, G. A. 1979. Experimental rabies in skunks: immunofluorescence light and electron microscopic studies. *Lab. Invest.* **41**: 36–44.
5. Charlton, K. M. and Casey, G. A. 1981. Experimental rabies in skunks: persistence of virus in denervated muscle at the inoculation site. *Can. J. Comp. Med.* **45**: 357–362.
6. Charlton, K. M., Nadin-Davis, S., Casey, G. A. and Wandeler, A. I. 1997. The long incubation period in rabies: delayed progression of infection in muscle at the site of exposure. *Acta Neuropathol.* **94**: 73–77.
7. Clem, R. J. and Miller, L. K. 1993. Apoptosis reduces both the *in vitro* replication and the *in vivo* infectivity of a baculovirus. *J. Virol.* **67**: 3730–3738.
8. Coulon, P., Derbin, C., Kucera, P., Lafay, F., Prehaud, C. and Flamand, A. 1989. Invasion of the peripheral nervous systems of adult mice by the CVS strain of rabies virus and its avirulent derivative AvO1. *J. Virol.* **63**: 3550–3554.
9. Gillet, J. P., Derer, P. and Tsiang, H. 1986. Axonal transport of rabies virus in the central nervous system of the rat. *J. Neuropathol. Exp. Neurol.* **45**: 619–634.
10. Guigoni, C. and Coulon, P. 2002. Rabies virus is not cytolytic for rat spinal motoneurons *in vitro*. *J. Neurovirol.* **8**: 306–317.
11. Harrison, A. K. and Murphy, F. A. 1978. Lyssavirus infection of muscle spindles and motor end plates in striated muscle of hamsters. *Arch. Virol.* **57**: 167–175.
12. Hemachudha, T., Wacharapluesadee, S., Lumlertdaecha, B., Orciari, L. A., Rupprecht, C. E., La-Ongpant, M., Juntrakul, S. and Denduangboripant, J. 2003. Sequence analysis of rabies virus in humans exhibiting encephalitic or paralytic rabies. *J. Infect. Dis.* **188**: 960–966.
13. Inoue, S., Sato, Y., Hasegawa, H., Noguchi, A., Yamada, A., Kurata, T. and Iwasaki, T. 2003. Cross-reactive antigenicity of nucleoproteins of lyssaviruses recognized by a monospecific antirabies virus nucleoprotein antiserum on paraffin sections of formalin-fixed tissues. *Pathol. Int.* **53**: 525–533.
14. Iwasaki, Y., Gerhard, W. and Clark, H. F. 1977. Role of host immune response in the development of either encephalitic or paralytic disease after experimental rabies infection in mice. *Infect. Immun.* **18**: 220–225.
15. Jackson, A. C. 1991. Biological basis of rabies virus neurovirulence in mice: comparative pathogenesis study using the immunoperoxidase technique. *J. Virol.* **65**: 537–540.
16. Jackson, A. C. and Park, H. 1998. Apoptotic cell death in experimental rabies in suckling mice. *Acta Neuropathol.* **95**: 159–164.
17. Jackson, A. C. and Rossiter, J. P. 1997. Apoptosis plays an important role in experimental rabies virus infection. *J. Virol.* **71**: 5603–5607.
18. Johnson, R. T. 1965. Experimental rabies. Studies of cellular vulnerability and pathogenesis using fluorescent antibody staining. *J. Neuropathol. Exp. Neurol.* **24**: 662–674.
19. Kucera, P., Dolivo, M., Coulon, P. and Flamand, A. 1985. Pathways of the early propagation of virulent and avirulent rabies strains from the eye to the brain. *J. Virol.* **55**: 158–162.
20. Lewis, P., Fu, Y. and Lentz, T. L. 2000. Rabies virus entry at the neuromuscular junction in nerve–muscle cocultures. *Muscle Nerve* **23**: 720–730.
21. Majno, G. and Joris, I. 1995. Apoptosis, oncosis, and necrosis. An overview of cell death. *Am. J. Pathol.* **146**: 3–15.
22. Morimoto, K., Hooper, D. C., Spitsin, S., Koprowski, H. and Dietzschold, B. 1999. Pathogenicity of different rabies virus variants inversely correlates with apoptosis and rabies virus glycoprotein expression in infected primary neuron cultures. *J. Virol.* **73**: 510–518.
23. Murphy, F. A. 1977. Rabies pathogenesis. *Arch. Virol.* **54**: 279–297.
24. Murphy, F. A. and Bauer, S. P. 1974. Early street rabies virus infection in striated muscle and later progression to the central nervous system. *Intervirology* **3**: 256–268.
25. Murphy, F. A., Bauer, S. P., Harrison, A. K. and Winn, W. C. 1973. Comparative pathogenesis of rabies and rabies-like viruses. Viral infection and transit from inoculation site to the central nervous system. *Lab. Invest.* **28**: 361–376.
26. Shankar, V., Dietzschold, B. and Koprowski, H. 1991. Direct entry of rabies virus into the central nervous system without prior local replication. *J. Virol.* **65**: 2736–2738.
27. Smith, J. S., Yager, P. A. and Baer, G. M. 1996. A rapid tissue culture test for determining rabies-neutralizing antibody. pp.371–373. *In*: Laboratory Techniques in Rabies, 4nd ed. (Meslin, F. X., Kaplan, M. M. and Koprowski, H. eds.), Geneva: World Health Organization.
28. Tang, Y., Rampin, O., Giuliano, F. and Ugolini, G. 1999. Spinal and brain circuits to motoneurons of the bulbospongiosus muscle: retrograde transneuronal tracing with rabies virus. *J. Comp. Neurol.* **414**: 167–192.
29. Theerasurakarn, S. and Ubol, S. 1998. Apoptosis induction in brain during the fixed strain of rabies virus infection correlates with onset and severity of illness. *J. Neurovirol.* **4**: 407–414.
30. Ugolini, G. 1995. Specificity of rabies virus as a transneuronal tracer of motor networks: transfer from hypoglossal motoneurons to connected second-order and higher order central nervous system cell groups. *J. Comp. Neurol.* **356**: 457–480.
31. Watson, H. D., Tignor, G. H. and Smith, A. L. 1981. Entry of rabies virus into the peripheral nerves of mice. *J. Gen. Virol.* **56**: 372–382.
32. Weiland, F., Cox, J. H., Meyer, S., Dahme, E. and Reddehase, M. J. 1992. Rabies virus neuritic paralysis: immunopathogenesis of nonfatal paralytic rabies. *J. Virol.* **66**: 5096–5099.

JOURNAL OF CLINICAL MICROBIOLOGY, Nov. 2005, p. 5555–5559 Vol. 43, No. 11
0095-1137/05/$08.00+0 doi:10.1128/JCM.43.11.5555–5559.2005


# New Criteria for Immunofluorescence Assay for Q Fever Diagnosis in Japan

A. Setiyono,[1,3] M. Ogawa,[1]* Y. Cai,[1] S. Shiga,[1] T. Kishimoto,[1] and I. Kurane[2]

*Laboratory of Rickettsia and Chlamydia,[1] and Department of Virology I,[2] National Institute of Infectious Diseases, 1-23-1 Toyama, Shinjuku-Ku, Tokyo 162-8640, Japan, and Laboratory of Pathology, Department of Parasitology and Pathology, Faculty of Veterinary Medicine, Bogor Agricultural University, Jl. Agatis, Kampus IPB Darmaga Bogor 16680, Indonesia[3]*

Received 26 October 2004/Returned for modification 24 January 2005/Accepted 9 August 2005

**A study was made to evaluate the cutoff value of indirect immunofluorescent-antibody (IFA) test for Q fever diagnosis in Japan. We used 346 sera, including 16 from confirmed Q fever cases, 304 from Japanese pneumonia patients, and 26 from negative cases. Thirteen sera from the confirmed Q fever cases with an immunoglobulin M (IgM) titer of ≥1:128 and/or IgG titer of ≥1:256 by the IFA test were positive by both enzyme-linked immunosorbent assay (ELISA) and Western blotting assay (WBA), whereas 298 sera from pneumonia patients and 26 negative sera with an IgM titer of ≤1:16 and an IgG titer of ≤1:32 by the IFA test were negative by both ELISA and WBA. In the proposed "equivocal area," with an IgM titer of ≥1:32 and ≤1:64 and/or an IgG titer of ≥1:64 and ≤1:128, we found 9 sera, 3 from confirmed Q fever cases and 6 from Japanese pneumonia patients, by the IFA test. Three sera from the confirmed Q fever cases and one of the sera from pneumonia patients were IgM and/or IgG positive by both ELISA and WBA. These results suggest that a single cutoff value for the IFA test may cause false-positive and false-negative results. In conclusion, this study showed that an "equivocal area" should be used for the IFA test rather than a single cutoff value and that sera in the equivocal area should be tested by additional serological assays for confirmation.**

Q fever is a zoonosis caused by *Coxiella burnetii*, an obligate intracellular rickettsial organism. The clinical manifestations of Q fever are readily divided into acute and chronic forms. The most common clinical presentation of acute Q fever in human is an influenza-like illness, often accompanied by pneumonia. The chronic Q fever form, particularly endocarditis, may appear several years after the primary episode (1, 2, 6, 21). Because the clinical presentation of the infection is not specific, serological confirmation is required for the diagnosis of Q fever. In Japan, the currently used serological method is the indirect immunofluorescent-antibody (IFA) test, and more recently, some attempts have been made to use other methods, such as the enzyme-linked immunosorbent assay (ELISA).

The unique characteristic of *C. burnetii* is its antigenic phase variation (17). Virulent phase I can be isolated from natural infection of humans or from laboratory infections of animals. Phase II develops during serial passage in an immunologically incompetent host, such as cell cultures or fertilized eggs (1). Serologically, anti-phase I antibodies are normally found at high levels only during the chronic form of the disease, whereas specific anti-phase II antibodies predominate primarily in acute Q fever (14).

The IFA test has previously been used to detect immunoglobulin M (IgM) antibodies in the sera of Q fever patients within the first 2 weeks of illness (8, 12). The estimation of anti-*C. burnetii* IgM antibody using the IFA test in a single serum sample has been proven useful in confirming acute infection in humans (8). The IFA method is more sensitive and specific than the complement fixation test; however, it is less sensitive than the ELISA (15). Therefore, the validation of the immunofluorescent threshold value for Q fever serology should be important for the establishment of the diagnosis.

Sodium dodecyl sulfate-polyacrylamide gel electrophoresis, followed by immunoblotting assay, has been used to identify the biologically important antigen in a complex mixture of proteins (9). The outer membrane-associated protein of *C. burnetii* is believed to be the antigenic target for the detection of antibody in clinical serum samples. This protein has been well characterized, with a molecular mass of approximately 27 kDa (18), and its usefulness as a immunodiagnostic reagent had also been evaluated (23).

In a preliminary study, we found some unsure results in the Q fever diagnosis by our IFA test and then compared them with ELISA results (data not published). Several samples reacted to phase II *C. burnetii* antigen in the IFA test but were negative by ELISA. On the other hand, a few of these sera were positive by ELISA but nonreactive in the IFA test. This phenomenon led us to reevaluate the criteria for the IFA test for the diagnosis of Q fever.

## MATERIALS AND METHODS

**Serum samples.** A total of 346 human serum samples were included in this study. The specimens consisted of 16 serum samples from patients diagnosed with Q fever in past examinations by the IFA test, ELISA, and complement fixation test, which also served as a positive control, including three imported cases (13) and others kindly provided by Werner Slenczka (Institut fur Virologie, Marburg, Germany), Barrie P. Marmion (Institute of Medical and Veterinary Science, Adelaide, Australia), and E. Kovacova (Institute of Virology, Slovak Academy of Sciences, Slovak Republic), 150 paired and 4 single sera from Japanese pneumonia patients in Okayama Prefecture with unknown fever and no clinical information regarding the microbes in those pneumonia cases, and 26

* Corresponding author. Mailing address: Laboratory of Rickettsia and Chlamydia, Department of Virology I, National Institute of Infectious Diseases, 1-23-1 Toyama, Shinjuku-Ku, Tokyo 162-8640, Japan. Phone: 81-3-5285-1111, ext. 2563. Fax: 81-3-5285-1208. E-mail: ogawam@nih.go.jp.

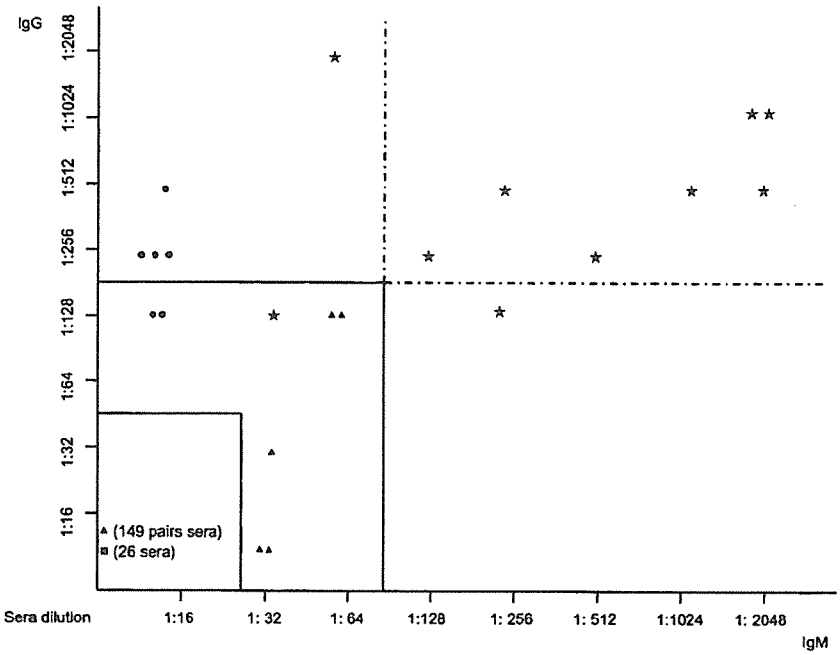


FIG. 1. Determination of IgM and IgG titers to phase II *C. burnetii* in 346 serum samples by immunofluorescence assay. ★, acute-phase sera from confirmed Q fever patients; ●, chronic- and convalescent-phase sera from confirmed Q fever patients; ▲, sera from Japanese pneumonia patients; ■, negative sera.

negative sera from healthy donors, including 1 serum sample from Slovakia and 25 sera from Japan.

***C. burnetii* antigen.** A total of $10^7$ *C. burnetii* phase II strain Nine Mile (ATCC VR615) bacteria with a high passage number were purified by differential centrifugation and formalin treatment as described previously (20), with minor modifications. Briefly, after 3 to 5 days of inoculation of *C. burnetii* to Vero cell lines, the medium was discarded and the cells were collected with a cell scraper. The cells were then resuspended by Dounce homogenization in 0.02% formalin–phosphate-buffered saline (PBS) (pH 7.2) 20 times. The cell solution was centrifuged at 1,300 × *g* for 5 min, and the supernatant was collected. Subsequently, the collected supernatant was filtered through a 5.0-μm-pore-size filter (Millipore Corp., Bedford, MA) to remove soluble cell culture debris and centrifuged at 13,000 × *g* at 4°C for 15 min. The supernatant was then discarded, and the pellets were washed with PBS twice. The concentration of *C. burnetii* antigen was measured with a Bio-Rad protein assay kit (Bio-Rad Lab., Hercules, CA). After microscopic examination of impression smears checked by the IFA test, the partially purified *C. burnetii* was pooled and stored at −80°C until use.

**IFA test.** The IFA test was performed by using prepared *C.burnetii* antigen with twofold dilutions of serum from 1:16 to 1:2,048 in PBS. In brief, 4 μl of antigen was dotted in triplicate onto a clean 15-well multitest slide (ICN Biomedicals, Inc., Aurora, Ohio) and allowed to air dry. Once dry, the slides were fixed in acetone for 15 min at room temperature. The diluted serum samples were then overlaid onto the antigen spots and incubated at 37°C in a humidified chamber for 1 h. After one wash with distilled water, two washes with 0.05% PBS–Tween, and one more wash with distilled water, 8 μl of fluorescein isothiocyanate-labeled anti-human IgM or IgG (Biosource, Camarillo, CA) diluted 1:200 in 0.001% Evans blue solution was added to each antigen spot and the slides were incubated for 1 h at 37°C. Finally, they were washed as before, dried in air, and mounted in 50% glycerol–PBS (pH 8.6). The slides were examined with a 40× objective (×400 magnification) using a fluorescence microscope (Axioskop 2 plus; Zeiss) equipped for visualizing brilliant green staining of *C. burnetii* microorganisms.

**ELISA.** A commercial ELISA kit (PanBio Co Ltd., Windsor, Queensland, Australia) was used as recommended by the manufacturer. The bound conjugates were detected by using tetramethyl benzidine as a substrate, and the color change was assessed in a microplate reader at a test wavelength of 450 nm. The ELISA index can be obtained by calculating the ratio of the cutoff absorbance to the sample absorbance and multiplying by 10. The serum samples were considered positive if they had an index of more than 11, equivocal if the index was between 9 and 11, and negative if the index was less than 9.

**WBA.** The outer membrane complex of *C. burnetii* was extracted by trichloroacetic acid and the temperature treatment method as described elsewhere (22). Sodium dodecyl sulfate-polyacrylamide gel electrophoresis was carried out with a 12% polyactylamide gel as a separating gel (12), and a Western blotting assay (WBA) was performed using prepared outer membrane complex with 1:400 dilutions of the sera. The assay result was considered positive if the sera recognized the approximately 27-kDa protein of *C. burnetii*.

TABLE 1. Grouping of results

| Group no. | Serum origin | No. of samples with result: | | | Total no. of: | |
|---|---|---|---|---|---|---|
| | | Q fever | Negative | Equivocal | Serum samples | Patients |
| 1 | Confirmed Q fever patients | 13 | | 3 | 16 | 16 |
| 2 | Japanese pneumonia patients | | 149 pairs | 1 pairs, 4 single | 304 | 150<br>4 |
| 3 | Negative samples | | 26 | | 26 | 26 |
| Total | | | | | 346 | 196 |

TABLE 2. Results of IFA test, ELISA, and Western blotting assay

| Subtype | Test | Assay result[a] | | | |
|---|---|---|---|---|---|
| | | Chronic- and convalescent-phase sera (4 samples) | Acute-phase sera (9 samples) | Negative | |
| | | | | 149 pairs of sera | 26 samples |
| IgM | IFA | — | + | — | — |
| | ELISA | — | + | — | — |
| | WBA | — | + | — | — |
| IgG | IFA | + | + | — | — |
| | ELISA | + | + | — | — |
| | WBA | + | + | — | — |

[a] +, positive; —, negative. Equivocal results were obtained for three samples from confirmed Q fever cases and six samples (one paired and four single sera) from Japanese pneumonia patients. See Table 3 for details regarding equivocal results.

## RESULTS

**Serological analysis.** Three hundred forty-six human sera, including 16 sera from confirmed Q fever cases, 304 sera from pneumonia patients, and 26 negative sera, were tested by the IFA test (Fig. 1), ELISA, and WBA (Table 1). Thirteen sera with an IgM titer of ≥1:128 and/or an IgG titer of ≥1:256 by the IFA test were positive by both ELISA and WBA, whereas 302 sera with an IgM titer of ≤1:16 and an IgG titer of ≤1:32 by the IFA test were negative by both ELISA and WBA. In the case of an IgM titer of ≥1:32 and ≤1:64 and/or an IgG titer of ≥1:64 and ≤1:128 by the IFA test, 4 sera were IgM and/or IgG positive by both ELISA and WBA, whereas 2 sera were negative by ELISA but positive by WBA. In this study, we labeled this area the "equivocal area" and divided the results of the IFA test into 3 groups, as shown in Table 1. The detailed results of the 3 groups are discussed in the next section.

**Groups.** Group I included 13 sera from confirmed Q fever cases. Four of these sera were IgG positive by both ELISA and WBA, indicating convalescent or chronic cases, whereas 9 of these sera were IgM and IgG positive by both ELISA and WBA, suggesting acute or subacute cases (Table 2). Group II included 298 sera from pneumonia patients and 26 confirmed negative sera that were negative by ELISA and WBA. Group III, which was proposed as the "equivocal area" in this study, included 3 sera from confirmed Q fever cases and 6 sera from pneumonia patients. The 3 confirmed Q fever sera and one serum from a pneumonia patient were IgM and/or IgG positive by both ELISA and WBA (Table 3). However, 2 of the sera from pneumonia patients were negative by ELISA but positive by WBA, and the other 3 sera were negative by both ELISA and WBA.

## DISCUSSION

We evaluated new criteria for the IFA test in the diagnosis of Q fever in Japan. We used 346 human sera, including 16 from confirmed Q fever cases, 304 from Japanese pneumonia patients, and 26 that were negative. Thirteen sera from the confirmed Q fever cases were positive by the IFA test, ELISA, and WBA, whereas 298 sera from pneumonia patients and 26 negative sera were negative by the IFA test, ELISA, and WBA. In the proposed "equivocal area," we found 9 sera with various results by the IFA test, ELISA, and WBA for each serum sample.

The high cutoff value should emphasize the predictive value of a positive result with a high probability. In our temporary criteria, the combination of a phase II IgM titer of ≥1:128 and/or a phase II IgG titer of ≥1:256 gave a positive result for 13 sera from confirmed Q fever patients. Under these conditions, the diagnosis can be made even with only a single serum sample. Additionally, the serum samples recognized an approximately 27-kDa protein of *C. burnetii* by WBA, which other workers suggested as an immunodominant component in certain acute cases of the disease (18, 19), and were positive by ELISA. These criteria can be considered more reliable than those of a recent study that defined the high sensitivity of the IFA test at a cutoff titer of 1:400 (16).

The low cutoff value for either IgM or IgG should give a high predictive value of a negative result; thus, diagnosis cannot be made below this titer with a high probability. We may consider phase II IgM and phase II IgG titers of ≤1:16 and ≤1:32, respectively, as the low cutoff values (Fig. 1). Most samples under the low cutoff values, including 149 paired and 26 negative-control sera, were negative and also did not recognize the

TABLE 3. Confirmation of equivocal IFA test results with ELISA and Western blot assay

| Subtype | Test | Result for sample no. with serum origin: | | | | | | | |
|---|---|---|---|---|---|---|---|---|---|
| | | Confirmed Q fever patients | | | Japanese pneumonia patients | | | | |
| | | 1 | 2 | 3 | 1[a] | 2 | 3 | 4[b] | 5[b] |
| IgM | IFA[c] | 32 | <16 | <16 | 32 | 32 | 32 | 64 | 64 |
| | ELISA[d] | + | — | — | + | — | — | — | — |
| | WBA[e] | + | — | — | + | — | — | + | + |
| IgG | IFA | 128 | 128 | 128 | <16 | <16 | <16 | 128 | 128 |
| | ELISA | + | + | + | — | — | — | — | — |
| | WBA | + | + | + | — | — | — | — | — |

[a] Probable acute case.
[b] Suspected acute case.
[c] The numbers show titers as twofold dilutions.
[d] +, positive, if the index was more than 11 units; —, negative, if the index was less than 9 units.
[e] +, positive, if sera recognized the approximately 27-kDa protein; —, negative, if sera did not recognize the protein.

TABLE 4. Confirmation of equivocal ELISA results with IFA test and Western blotting assay

| Subtype | Test | Result for indicated sample no. with serum origin: Confirmed Q fever patients | | | | Japanese clinical specimen | | | | | | | | | | | | | |
|---|---|---|---|---|---|---|---|---|---|---|---|---|---|---|---|---|---|---|---|
| | | 1 | 2 | 3 | 4 | 1[a] | 2 | 3 | 4 | 5 | 6 | 7 | 8 | 9 | 10 | 11 | 12 | 13 | 14 |
| IgM | ELISA[b] | 15.1 | 13.8 | 8.3 | 8.8 | 12.8 | 14 | 12.5 | 3.4 | 7.3 | 7.9 | 10.4 | 4.2 | 8.3 | 13.5 | 11.1 | 11.2 | 15.7 | 5.1 |
| | IFA[c] | 32 | + | <16 | <16 | 32 | <16 | <16 | <16 | <16 | <16 | <16 | <16 | <16 | <16 | <16 | <16 | <16 | <16 |
| | WB[d] | + | + | — | — | + | — | — | — | — | — | — | — | — | — | — | — | — | — |
| IgG | ELISA | 14.7 | 14 | 15.1 | 14.7 | 9.7 | 4.3 | 5.2 | 15.8 | 13 | 14.8 | 11.9 | 19.4 | 14.1 | 4.1 | 2.7 | 4.5 | 4.6 | 12.2 |
| | IFA | 128 | + | 128 | + | <16 | 32 | <16 | <16 | <16 | <16 | <16 | <16 | <16 | <16 | <16 | <16 | <16 | <16 |
| | WB | + | + | + | + | — | — | — | — | — | — | — | — | — | — | — | — | — | — |

[a] Probable acute case.
[b] The numbers indicate the ELISA index.
[c] The numbers indicate the IFA titer of the diluted sera (see details in the text).
[d] +, positive; −, negative in the recognition of the approximately 27-kDa protein.

specific protein by WBA, although a few of them had a significant index by ELISA (Table 4). This is in accordance with a previous study showing that ELISA is suitable for use as a screening assay for Q fever diagnosis, with the IFA test used to confirm negative results (3, 4). We may explain this difference by the fact that a nonspecific reaction by ELISA may still occur due to cellular debris in the antigen preparation from culture. Although a recent study showed that LightCycler nested PCR can also be applied as a secondary tool in the diagnostic strategy for the early diagnosis of acute Q fever (5), the result of this study showed a good correlation between IFA titers and ELISA index values. A higher IFA titer correlated with a higher index in the ELISA result. Based on this clarification, confirmation with another serological test might not be required for samples categorized as negative by the IFA test.

We proposed the titer equivocal area and found 9 sera, including 3 from confirmed Q fever cases and 6 from Japanese pneumonia patients in the area, by the IFA test. Three sera from the confirmed Q fever cases and one serum from a pneumonia patient were positive by ELISA and WBA. However, 2 sera from pneumonia patients were negative by ELISA but positive by WBA, which left 3 sera negative by both ELISA and WBA. These results suggest that a single cutoff value for the IFA test may cause false-positive and false-negative results. In addition, only the IgM titer was positive, and the titer was very low in the positive case of pneumonia. This result suggests that serological assay with paired sera should be done for confirmation.

The results presented here illustrate the new criteria for the IFA test for Q fever. We recommended that an "equivocal area" should be used for the IFA test, rather than a single cutoff value and that sera in the equivocal area should be tested by additional serological assays to eliminate false-positive and false-negative results.

## ACKNOWLEDGMENTS

We thank all the physicians who kindly provided the clinical samples for this study and Werner Slenczka, Barrie P. Marmion, and Elena Kovacova for kindly providing the control human sera.

This work was financially supported by The Japan Human Sciences Foundation.

## REFERENCES

1. **Baca, O. G., and D. Paretsky.** 1983. Q fever and *Coxiella burnetii*: a model for host-parasite interactions. Microbiol. Rev. **47**:127–149.
2. **Brouqui, P., H. Tissot Dupont, M. Drancourt, Y. Berlan, J. Etienne, C. Leport, F. Goldstein, P. Massip, M. Micoud, A. Bertrand, and D. Raoult.** 1993. Chronic Q fever: 92 cases from France including 27 cases without endocarditis. Arch. Intern. Med. **153**:642–648.
3. **Field, P. R., J. L. Mitchell, A. Santiago, D. J. Dickeson, S.-W. Chan, D. W. T. Ho, A. M. Murphy, A. J. Cuzzubbo, and P. L. Devine.** 2000. Comparison of a commercial enzyme-linked immunosorbent assay with immunofluorescence and complement fixation tests for detection of *Coxiella burnetii* (Q fever) immunoglobulin M. J. Clin. Microbiol. **38**:1645–1647.
4. **Field, P. R., A. Santiago, S.-W. Chan, D. B. Patel, D. Dickeson, J. L. Mitchell, P. L. Devine, and A. M. Murphy.** 2002. Evaluation of a novel commercial enzyme-linked immunosorbent assay detecting *Coxiella burnetii*-specific immunoglobulin G for Q fever prevaccination screening and diagnosis. J. Clin. Microbiol. **40**:3526–3529.
5. **Fournier, P. E., and D. Raoult.** 2003. Comparison of PCR and serology assays for early diagnosis of acute Q fever. J. Clin. Microbiol. **41**:5094–5098.
6. **Haldane, E. V., T. J. Marrie, R. S. Faulkner, S. H. Lee, J. H. Cooper, D. D. MacPherson, and T. J. Montague.** 1983. Endocarditis due to Q fever in Nova Scotia: experience with five patients in 1981–1982. J. Infect. Dis. **148**:978–985.
7. **Hendrix, L. R., L. P. Mallavia, and J. E. Samuel.** 1993. Cloning and sequencing of *Coxiella burnetii* outer membrane protein gene *com1*. Infect. Immun. **61**:470–477.
8. **Hunt, J. G., P. R. Field, and A. M. Murphy.** 1983. Immunoglobulin responses to *Coxiella burnetii* (Q fever): single-serum diagnosis of acute infection, using an immunofluorescence technique. Infect. Immun. **39**:977–981.
9. **Kenneth, O., and K. M. Yamada.** 1977. Direct detection of antigens in sodium dodecyl sulfate-polyacrylamide gels. Anal. Biochem. **78**:483–490.
10. **Kovacova, E., J. Gullo, S. Schramek, J. Kazar, and R. Brezina.** 1987. *Coxiella burnetii* antigens for detection of Q fever antibodies by ELISA in human sera. Acta Virol. **31**:254–259.
11. **Laemmli, U. K.** 1970. Cleavage of structural proteins during the assembly of the head of bacteriophage T4. Nature **227**:680–685.
12. **Murphy, A. M., and L. Magro.** 1980. IgM globulin response in Q fever (*Coxiella burnetii*) infections. Pathology **12**:391–396.
13. **Ogawa, M., T. Kawamoto, A. Kawamoto, T. Yamashita, Y. Uchida, K. Kato, A. Setiyono, S. Shiga, and T. Kishimoto.** 2003. Time course of the levels of antibodies to *Coxiella burnetii* and detection of *C. burnetii*-DNA in three imported cases of acute Q fever. Kansenshogaku Zasshi **77**:127–132. (In Japanese.)
14. **Peacock, M. G., R. N. Philip, J. C. Williams, and R. S. Faulkner.** 1983. Serological evaluation of Q fever in humans: enhanced phase I titers of immunoglobulins G and A are diagnostic for Q fever endocarditis. Infect. Immun. **41**:1089–1098.
15. **Peter, O., G. Dupuis, W. Burgdorfer, and M. Peacock.** 1985. Evaluation of complement fixation and indirect immunofluorescence tests in the early diagnosis of primary Q fever. Eur. J. Clin. Microbiol. **4**:394–396.
16. **Rollain, J. M., C. Lecam, and D. Raoult.** 2003. Simplified serological diagnosis of endocarditis due to *Coxiella burnetii* and *Bartonella*. Clin. Diagn. Lab. Immunol. **10**:1147–1148.
17. **Stocker, M. G. P., and P. Fiset.** 1956. Phase variation of the Nine Mile and other strains of Rickettsia burnetii. Can. J. Microbiol. **2**:310–321.
18. **To, H., A. Hotta, G. Q. Zhang, S. V. Nguyen, M. Ogawa, T. Yamaguchi, H. Fukushi, K. Amano, and K. Hirai.** 1997. Antigenic characteristics of polypeptides of *Coxiella burnetii* isolates. Microbiol. Immunol. **42**:81–85.
19. **To, H., A. Hotta, T. Yamaguchi, H. Fukushi, and K. Hirai.** 1997. Antigenic characteristics of the lipopolysaccharides of *Coxiella burnetii* isolates. J. Vet. Med. Sci. **60**:267–270.
20. **To, H., K. K. Htwe, N. Yamasaki, G. Q. Zhang, M. Ogawa, T. Yamaguchi, H.**

**Fukushi, and K. Hirai.** 1995. Isolation of *Coxiella burnetii* from dairy cattle and ticks, and some characteristics of the isolates in Japan. Microbiol. Immunol. **39**:663–671.
21. **Turk, W. P., G. Howitt, L. A. Turnberg, H. Fox, M. Longson, M. B. Matthews, and R. DasGupta.** 1976. Chronic Q fever. Q. J. Med. **45**:193–217.
22. **Vavrekova, M., F. Ciampor, and M. Lukacova.** 1992. Electron-microscopic study of the effect of various extractants on the morphology of *Coxiella burnetii*. Folia Microbiol. **37**:87–92.
23. **Zhang, G. Q., A. Hotta, T. Ho, T. Yamaguchi, H. Fukushi, and K. Hirai.** 1998. Evaluation of a recombinant 27-kDa outer membrane protein of *Coxiella burnetii* as an immunodiagnostic reagent. Microbiol. Immunol. **42**:423–428.